Silva Dos Santos, A. P. *et al.* (2010). *Géotechnique* **60**, No. 10, 791–799 [**doi:** 10.1680/geot.8.P.159]

The mechanics of fibre-reinforced sand

A. P. SILVA DOS SANTOS*, N. C. CONSOLI* and B. A. BAUDET†

Fibres can be an effective means of reinforcing soils. This paper presents data from laboratory triaxial tests on quartzitic sand reinforced with polypropylene fibres. By keeping the studied composite consistent throughout the study (host sand and fibre characteristics kept constant), it has been possible to develop a framework of behaviour for the sand–fibre material, which provides a solid base for future research on fibre-reinforced soils. Data from previous work and from new tests have been analysed within the Critical State framework, that is in terms of normal compression line, critical state line and state boundary surface.

KEYWORDS: laboratory tests; reinforced soils; sands

Les fibres sont parfois un moyen de renforcement efficace des sols. La présente communication présente des données issues d'essais triaxiaux en laboratoire sur un sable quartzique renforcé aux fibres de polypropylène. En maintenant l'homogénéité du composite étudié tout au long de l'étude (en maintenant constantes les propriétés du sable hôte et des fibres), il a été possible de développer un cadre de comportement pour la matière sable–fibre, qui constitue une fondation solide pour une recherche future sur les sols renforcés à la fibre. On a analysé des données provenant de travaux précédents et découlant d'essais nouveaux dans le cadre de l'état critique, autrement dit sur le plan de la ligne de compression, de la ligne de l'état critique, de la surface limite de l'état.

INTRODUCTION

Fibres can be an effective means of reinforcing soils. The effectiveness of fibre reinforcement will depend on the deformation characteristics of the host soil as well as the fibre properties (e.g. nature of fibres, fibre length, fibre aspect ratio) and the fibre content. The interaction between fibres and soil occurs at the particle level, yet the reinforced soil is to be used on much larger scales. Recent studies have attempted to model the soil and fibres using the discrete element method (e.g. Maeda & Ibraim, 2008), but to be usable in practice the behaviour of the soil reinforced with fibres must be characterised in terms of parameters for continuum mechanics. This can be achieved to a certain extent by studying the reinforced soil in laboratory element tests before developing a model to be implemented in finite-element analyses, for example, in the same approach that has been used for some time for non-reinforced soils.

Studies reported in the literature (e.g. Gray & Ohashi, 1983; Gray & Al-Refeai, 1986; Maher & Ho, 1993; 1994; Crockford *et al.*, 1993; Santoni *et al.*, 2001; Consoli *et al.*, 2009a) have generally been conducted independently and have not always been consistent, with the consequence that for a topic so wide it has been difficult to build a unified framework that could be linked to other recognised frameworks, for example, the critical state framework (Schofield & Wroth, 1968). When compiling these studies several facts can be advanced for sand–fibre composites. First, researchers seem to agree that the fibre content has a positive effect on the composite strength up to a certain percentage, after which no further effect is observed (Gray & Ohashi, 1983; Gray & Al-Refeai, 1986; Maher & Ho, 1994; Santoni *et al.*, 2001). Similarly, an increase in the fibre length gives a gain in resistance of the reinforced material, but this gain reduces asymptotically after a threshold fibre length (Gray & Ohashi, 1983; Santoni *et al.*, 2001). In terms of post-peak resistance, there is a consensus that the addition of fibres to soil reduces the loss in strength post-peak (e.g. Gray & Al-Refeai, 1986; Ranjan & Charan, 1996; Consoli *et al.*, 1997; 1999; 2003a; 2007a; Casagrande *et al.*, 2006) but has the effect of increasing the amount of volumetric compression at rupture (Bueno *et al.*, 1996; Stauffer & Holtz, 1996), the higher the fibre content the larger the volumetric deformation (Shewbridge & Sitar, 1989; Nataraj *et al.*, 1996). As far as installation is concerned, using randomly distributed fibres has the advantage of avoiding any plane of weakness (Gray & Al-Refeai, 1986; Gray & Maher, 1989), even though in specimens prepared using moist tamping the fibres may not retain an isotropic distribution (Diambra *et al.*, 2008).

The studies reported above mainly aimed at assessing the effects of varying fibre properties and fibre content on the composite performance. There is, however, a gap between our understanding of the behaviour of the host soil and that of the fibre-reinforced soil, which renders modelling sand–fibre composites very difficult. In order to understand and characterise the behaviour of fibre-reinforced soil with respect to other known behaviours, the behaviour of the host soil being an obvious reference point, one should avoid dealing with too many variables and start with a unique composite. This paper presents data from laboratory tests on quartzitic sand reinforced with polypropylene fibres. By keeping the studied composite consistent throughout the study (host sand and fibre characteristics kept constant), it has been possible to develop a framework of behaviour for the sand–fibre material, which provides a solid base for future research on fibre-reinforced soils. The work presented here is the result of many years of research, some parts of it already published, but for the first time results from tests covering a wide range of stresses and strains have enabled the authors to find steady states in agreement with the definition of critical state in volume as well as stress space.

MATERIAL, TESTING PROGRAMME AND PROCEDURES

The sand–fibre composite used in this study, which is made of fine quartzitic Osorio sand and polypropylene fibres, has been investigated extensively over the past 14 years at

Manuscript received 17 December 2008; revised manuscript accepted 26 November 2009. Published online ahead of print 12 May 2010.
Discussion on this paper closes on 1 March 2011, for further details see p. ii.
* Federal University of Rio Grande do Sul, Brazil.
† Department of Civil Engineering, University of Hong Kong;

the Federal University of Rio Grande do Sul (UFRGS, Brazil) using mainly laboratory element tests (triaxial and ring shear tests) (Consoli *et al.*, 1998; 2002; 2003b; 2003c; 2004; 2005; 2007b; 2009b; Heineck *et al.*, 2005; Specht *et al.*, 2006; Santos, 2008).

Material tested

Laboratory tests were performed on pure sand, and sand reinforced with fibres. The host sand was Osorio sand, recovered from the Osorio region in Rio Grande do Sul, Brazil. It can be described as a fine, clean quartzitic sand with a uniform grading. The characteristics of the Osorio sand are given in Table 1.

The fibres used are short filaments made of polypropylene. They are chemically inert and have uniform characteristics, with a relative density of 0·91, a tensile resistance of 120 MPa, an elastic modulus of 3 GPa and a range of linear deformation at rupture between 80% and 170%. The dimensions of the fibres used in the tests were 0·023 mm in diameter and 24 mm long. The reinforced samples had a fibre content of 0·5% by weight.

Although no method has been agreed to determine the maximum and minimum void ratios for fibre-reinforced sand, there is evidence that the values can be very different and higher than that for the sand (Casagrande, 2005). Using the same procedure as that used to determine $e_{max} = 0{\cdot}90$ and $e_{min} = 0{\cdot}60$ in pure sand (NBR 12004-ABNT (ABNT, 1990)), values of $e_{max} = 0{\cdot}95$ and $e_{min} = 0{\cdot}65$ were obtained for the fibre-reinforced sand.

Testing programme and procedures

Most data presented here were obtained by Santos (2008), at the UFRGS in Brazil, and at Imperial College London. Two similar series of isotropically consolidated drained (CID) triaxial tests were carried out on specimens of sand and of fibre-reinforced sand. The confining pressure, ranging from 100 kPa to 5400 kPa, was kept constant during the tests. Two isotropic compression tests were also performed on the Osorio sand to provide a reference normal compression line (NCL_{sand}). Isotropic compression data for the reinforced sand were previously obtained by Consoli *et al.* (2005); they are used in the present analyses. Additional data obtained by Consoli *et al.* (2007a) on fibre-reinforced sand are also shown to help complete the overall picture of behaviour. These latter tests (under distinct stress paths) were carried out using Bishop & Wesley (1975) triaxial cells with internal and external measurement of strains, and were typically stopped at shear strains between 20% and 28%, without always reaching critical state. It is thus with caution that they are used in the following. A summary of the tests is given in Table 2.

Table 1. Properties of Osorio sand

Properties	Osorio sand
Specific gravity of solids	2·62
Uniformity coefficient, C_u	2·1
Curvature coefficient, C_c	1·0
Effective diameter, D_{10}: mm	0·09
Mean diameter, D_{50}: mm	0·16
Minimum void ratio, e_{min}	0·6
Maximum void ratio, e_{max}	0·9

The new data presented here (from the thesis by Santos (2008)) were obtained from triaxial CID tests carried out in a Bishop & Wesley (1975) cell equipped with a pressure multiplier for confining pressures up to 1200 kPa, and a 100 kN Wykeham Farrance frame with a reinforced triaxial chamber for tests using confining pressures up to 7 MPa. Local strains were measured using inclinometers (Burland & Symes, 1982) and linear variable differential transducers (LVDTs). The isotropic compression tests were performed in a high-pressure triaxial apparatus capable of applying up to 70 MPa confining stress (Cuccovillo & Coop, 1999). The particle size distributions of the Osorio sand were monitored by dry sieve and hydrometer testing before and after testing, in the pure sand and the fibre-reinforced sand specimens, having previously separated fibres and sands. The specimens were prepared using a set of constant variables: a fibre length of 24 mm, fibre diameter of 0·023 mm, fibre content of 0·5% by weight of soil and an initial moisture content of 10%. These values were chosen based on previous studies carried out at the Federal University of Rio Grande do Sul. Specimens 38 mm in diameter and 76 mm long were prepared for the tests performed at confining pressures up to 1200 kPa, and specimens 50 mm diameter and 100 mm long were prepared for the tests at higher pressures, up to 7000 kPa. For the fibre length selected and these sizes of specimens, accumulated experience of working with fibre-reinforced sand has indeed shown that boundary effects can be neglected. The specimens were compacted in three layers in a three-part mould under a vacuum pressure of 20 kPa, while controlling the weight so as to achieve the required density. The end platens were lubricated to avoid friction. After the tests, the specimens were dissected and the length of the fibres was recorded to monitor eventual elongation or rupture. The test data reported are in terms of triaxial invariants: the deviator stress $q = \sigma'_a - \sigma'_r$, the mean effective stress $p' = (1/3)(\sigma'_a + 2\sigma'_r)$. Strains are given as the volumetric strain $\varepsilon_v = \varepsilon_a + 2\varepsilon_r$, and the shear strain $\varepsilon_s = (2/3)(\varepsilon_a - 2\varepsilon_r)$. Because of the magnitude of the strains reached, in all cases these are natural (true) strains ε_n calculated from the measured linear strains ε_l

$$\varepsilon_n = -\ln(1 - \varepsilon_l) \quad (1)$$

Table 2. Tests used in the analyses

Material	Type of test	Confining stress: kPa	No. of tests	Reference
Sand	Isotropic compression	Up to 45 000	2	Santos (2008)
	Triaxial compression	100; 800; 3400; 5400	9	Santos (2008)
	Triaxial compression	20; 100; 200; 400	4	Consoli *et al.* (2007a)
Sand–fibre	Isotropic compression	Up to 50 000	2	Consoli *et al.* (2005)
	Triaxial compression	100; 800; 3400	5	Santos (2008)
	Triaxial compression	20*; 100; 400	3	Consoli *et al.* (2007a)
	Stress path $dq/dp' = -3$	20; 100	2	Consoli *et al.* (2007a)
	Constant p'	20; 100	2	Consoli *et al.* (2007a)

* Still dilating at end of shearing.

BEHAVIOUR DURING ISOTROPIC COMPRESSION

Results from isotropic compression tests on sand only, and sand reinforced with fibres, are shown in Fig. 1. There seem to be two distinct and parallel NCLs, the NCL for the reinforced soil ($NCL_{sand–fibre}$) lying to the right of the NCL for the sand only. Similar results were indeed found by Consoli *et al.* (2005), who proposed linear equations for the NCL of the host Osorio sand, fitted from post-yield data from a unique isotropic compression test

$$v = 2{\cdot}98 - 0{\cdot}156 \ln p' \tag{2}$$

And to the isotropic compression line for the sand reinforced with fibres

$$v = 3{\cdot}09 - 0{\cdot}156 \ln p' \tag{3}$$

The location of the NCL of the fibre–sand mixture above the NCL of the sand might be due to a lock-in effect of the fibres, therefore allowing a larger void ratio to exist in the composite material, which is not removed at large compressive stresses and large volumetric strains.

The NCL_{sand} and $NCL_{sand–fibre}$ appear to be curved at lower stresses. In pure sand, it is accepted that there is a range of void ratios at which the sand can exist, defined by its packing capability. Existing constitutive models for sands often distinguish between the first loading curve, which has been found to be curved for many sands, and the NCL, attained at very high stresses (Pestana & Whittle, 1999; Jefferies & Been, 2000). Because the shearing tests presented below were performed at confining stresses ranging from very low (20 kPa) to very high (5400 kPa), it was decided to fit a curved equation to the NCL_{sand} and $NCL_{sand–fibre}$. The equations chosen were based on the constitutive law proposed by Gudehus (1996) to describe changes in states of granular materials. A similar approach had been successfully used by Klotz & Coop (2001). This expression presents the advantage that while it has been derived from micromechanical principles, it comports very few parameters, all reasonably well defined or at least varying within a restricted range defined by boundary values. The equation is expressed as follows

$$v = 1 + e_0 \exp\left[-\left(\frac{3p'}{h_s}\right)^n\right] \tag{4}$$

where e_0 is the maximum global void ratio, n is a constant exponent ($0{\cdot}3 < n < 0{\cdot}5$) and the granular hardness h_s represents the compliance of the grain skeleton. The values e_0, n and h_s were chosen to best fit the data points obtained from the tests. The same value of $n = 0{\cdot}55$ and hardness $h_s = 180\,000$ kPa were selected for the sand and sand–fibre composite, assuming that adding fibres does not change these parameters. The maximum void ratios were taken to be different, as volumetric data seem to suggest in Fig. 1. The value of maximum void ratio $e_0 = 0{\cdot}90$ was used for the sand, and the value of maximum void ratio $e_0 = 0{\cdot}95$ determined as described above was used for the fibre-reinforced sand. These curves will be used later to normalise the shearing data and identify state boundary surfaces.

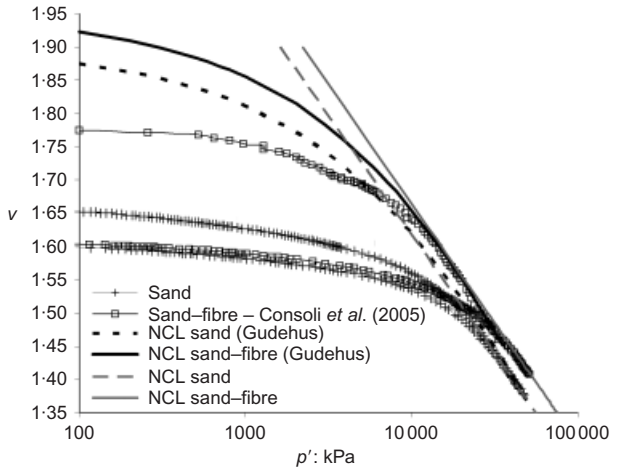

Fig. 1. Isotropic compression data and NCLs for sand and fibre-reinforced sand

BEHAVIOUR DURING TRIAXIAL SHEARING

In previous studies of the Osorio sand–polypropylene fibres composite, the sand–fibre material was found to show higher strength at higher strains, when a greater mobilisation of the tensile resistance of the fibres allowed a greater contribution of the fibres to the rigidity of the composite (Heineck *et al.*, 2005). No effect of the fibre reinforcement could be detected at very small strains, while at large strains there was no tendency to lose strength (Heineck *et al.*, 2005; Consoli *et al.*, 2007b). A series of triaxial compression tests under distinct stress paths indicated that the failure envelope of the fibre-reinforced sand is independent of stress path, and that it is bilinear with a noticeable kink (Consoli *et al.*, 2007a). The kink was attributed to a change of mechanism at the fibre–soil interface, from a phase where the fibres slip and yield, to a phase where all fibres have yielded and are stretched, following Gray & Ohashi (1983), Gray & Al-Refeai (1986), Maher & Gray (1990) and Consoli *et al.* (2007a).

Stress–strain and volumetric response during shearing

Specimens of non-reinforced and reinforced sand were isotropically consolidated to pressures varying between 100 kPa and 5400 kPa before shearing drained while keeping the cell pressure constant. The stress–strain response during shearing is shown in Fig. 2. The ranges of initial fabrication void ratios used for the pure sand and sand–fibre specimens were similar, varying between 0·66 and 0·81 for the pure sand, and between 0·69 and 0·82 for the reinforced sand. In the fibre-reinforced sand, these values represent the global void ratio. It was not possible to create denser or looser specimens because of difficulties encountered in moulding the specimens, while trying to ensure reproducibility between samples. As expected, the denser pure sand specimens showed a peak strength, and the looser specimens strain-hardened to critical state. In contrast, all fibre-reinforced specimens were found to strain-harden to reach a steady strength, irrespective of the initial void ratio. The effect of the fibres on this strength seems to depend on the testing confining pressure, reducing with increasing confining stress: in tests carried out at low (100 kPa) confining pressure, the shear strength of the reinforced sand is calculated to be about three to four times that of the pure sand (Fig. 2(a)), while at higher confining pressures, the gain in shear strength is reduced to only about 70% at 800 kPa (Fig. 2(b)), and 15% at 3400 kPa confining pressure (Fig. 2(c)). There seems also to be an effect of the specimen density, as sand–fibre specimens sheared under the same confining pressure do not necessarily reach the same strength. Similar results have been reported for ring shear tests in similar mixtures of sand and fibres (Consoli *et al.*, 2007b) but no explanation could be given.

The effect of the fibres on the volumetric response during shearing is not as clear. At 100 kPa confining pressure, the fibres seem to increase the initial compression while inhibiting the following dilation (Fig. 2(a)). At higher confining

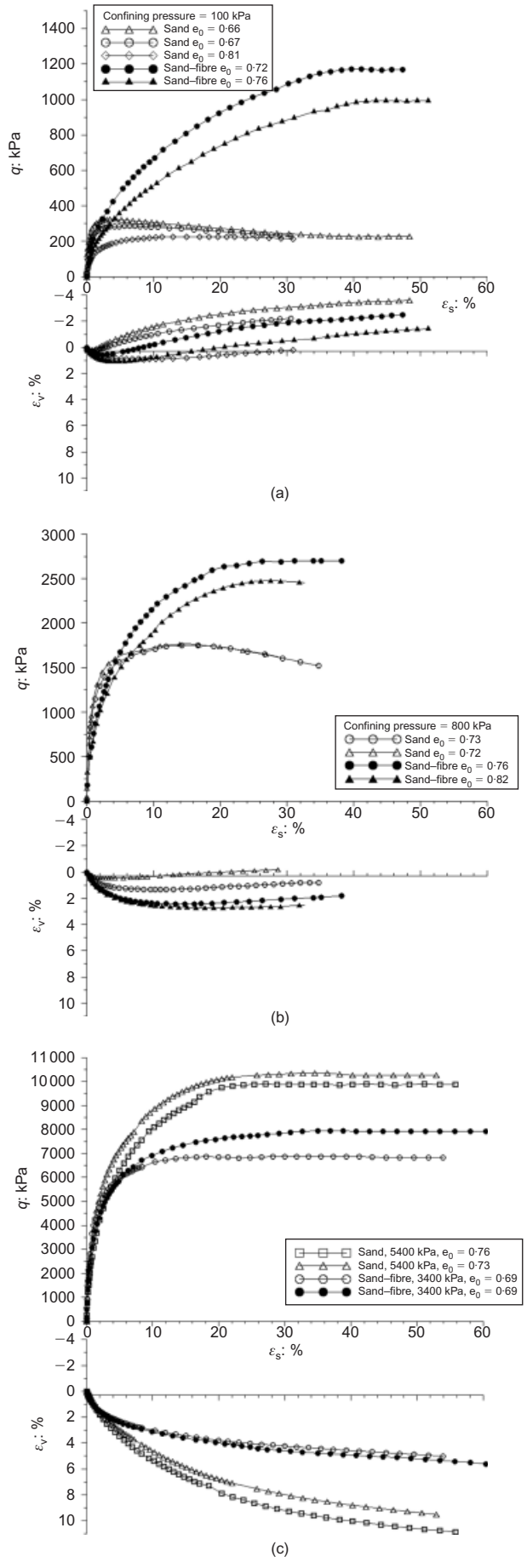

Fig. 2. Stress–strain–volumetric response of sand and fibre-reinforced sand for confining pressures of (a) 100 kPa; (b) 800 kPa; and (c) 3400 kPa and 5400 kPa

pressures, very little effect is observed, for example, the volumetric curves of the two specimens of sand and sand–fibre starting at a void ratio $e_0 = 0{\cdot}69$ in Fig. 2(c) are almost coincident. Similar results for the same sand and fibre were found by Consoli *et al.* (2007a) for different confining pressures and stress paths. This is better explained by looking at the stress–dilatancy behaviour, detailed in the following section.

Stress–dilatancy

Figure 3 compares the stress–dilatancy behaviour of pure sand (Fig. 3(a)) and reinforced sand (Fig. 3(b)). For the pure sand, all specimens sheared at high confining stresses compress to critical state, with the rate of compression decreasing with increasing stress ratio until the critical state ratio (here $M = 1{\cdot}22$) is reached. Only the denser specimen tested at 100 kPa confining stress, with a fabrication void ratio $e_0 = 0{\cdot}66$, showed a clear dilation up to a peak dilation rate and stress ratio, before reducing to reach the critical state ratio of $M = 1{\cdot}22$. In Fig. 3(b), which shows data for the sand–fibre material, the trend is very different. The stress–dilatancy behaviour is more uniform in compression, and less dependent on the initial void ratio than for the pure sand. The confining pressure seems to influence the dilatancy behaviour: at lower confining stress levels, the compression does not stop at reaching a rate of volumetric change $\delta\varepsilon_v/\delta\varepsilon_s = 0$, but is followed by a small dilation, which then reduces to reach a stress state ratio equal to 2·4. Thus at lower confining stresses, the inclusion of fibres increases the peak stress ratio, but unlike for pure sand, this peak stress ratio does not correspond to the maximum rate

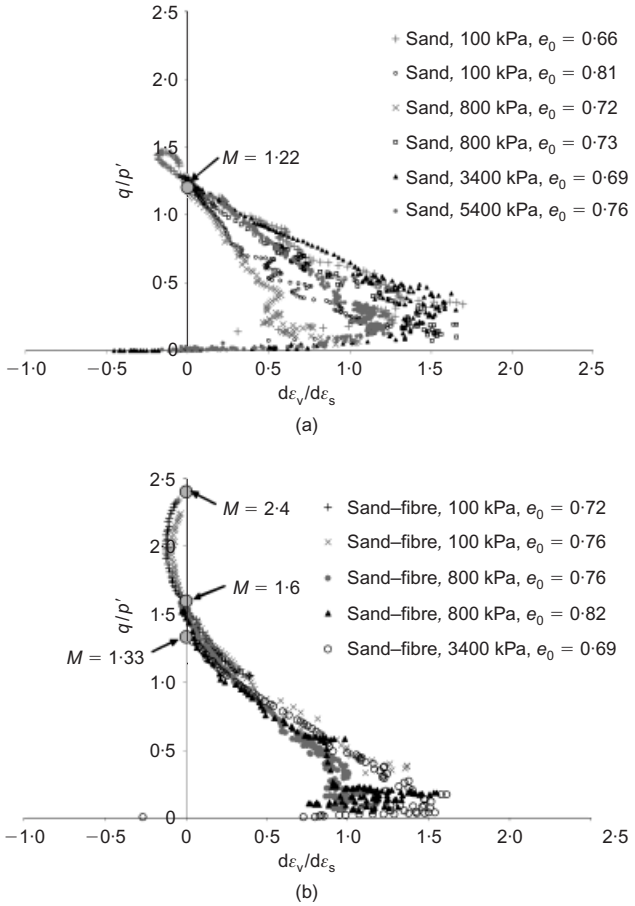

Fig. 3. Stress–dilatancy response of (a) sand and (b) fibre-reinforced sand

of dilation, and rather seems to be reached at the end of dilation. At higher confining pressures, this dilation behaviour disappears so the sand–fibre composite only compresses to a stress state ratio equal to 1·33–1·6 that seems to be increasingly independent of stress level, as would be observed on pure sand. Unlike the pure sand, however, the compressive part of the stress–dilatancy does not depend on stress level, with approach paths forming a narrow band.

MECHANICS OF FIBRE–SAND COMPOSITE

Because of the high stresses reached during isotropic compression, of the order of 50 MPa, particle breakage was monitored by comparing the particle size distribution of the sand before and after test. The grading tests were repeated several times. Fig. 4 shows the average grading curve obtained: it shifted upwards during testing as a result of compression of the pure sand, signalling that particle breakage did occur. The particle size distribution of the fibre-reinforced sand, which was compressed to similar stresses, was also determined after testing from repeated grading tests. When compared to the grading of the pure sand after testing, it appears that the fibres may have curtailed breakage in the fibre–sand composite. It is difficult to advance what may have happened at particle level. One hypothesis could be that the energy lost in deforming and breaking the fibres is reducing energy for crushing the particles; another hypothesis could be that the fibres, by enveloping some of the grains, contribute to reducing abrasion.

The initial fibre length distribution, that is determined before any testing, is presented in Fig. 5(a). The distribution of fibre lengths in Fig. 5(b), which was determined after the isotropic compression test to 50 MPa by Consoli *et al.* (2005), indicates that only about 20% of the fibres retained their original length. The remaining fibres were found either to have broken into smaller length fibres (~50%), or to have elongated (~30%). The existence of a minimum value of 14 mm for the length of the broken fibres suggests that the fibres were broken under tension rather than by pinching, so that the fibres acted in tension even when undergoing large compressive volume strains. The maximum fibre length recorded after elongation is 35 mm, which corresponds to about 50% elongation. This is less than the maximum elongation of 170% that the fibres are supposed to be able

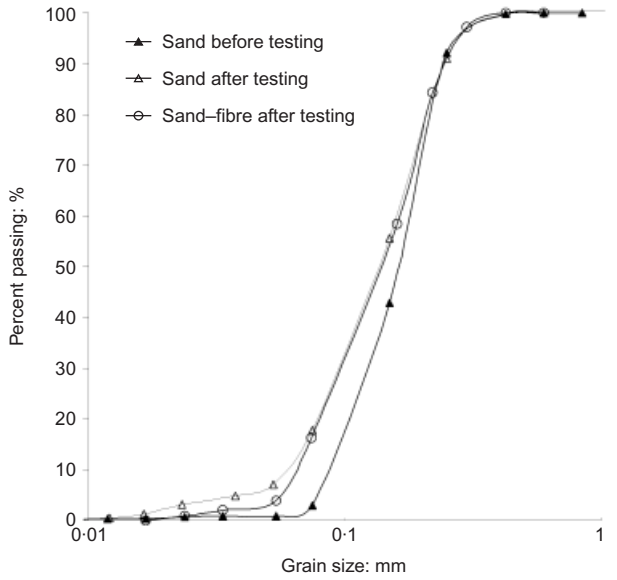

Fig. 4. Evolution of grading during isotropic compression to about 50 MPa for sand and sand–fibre specimens

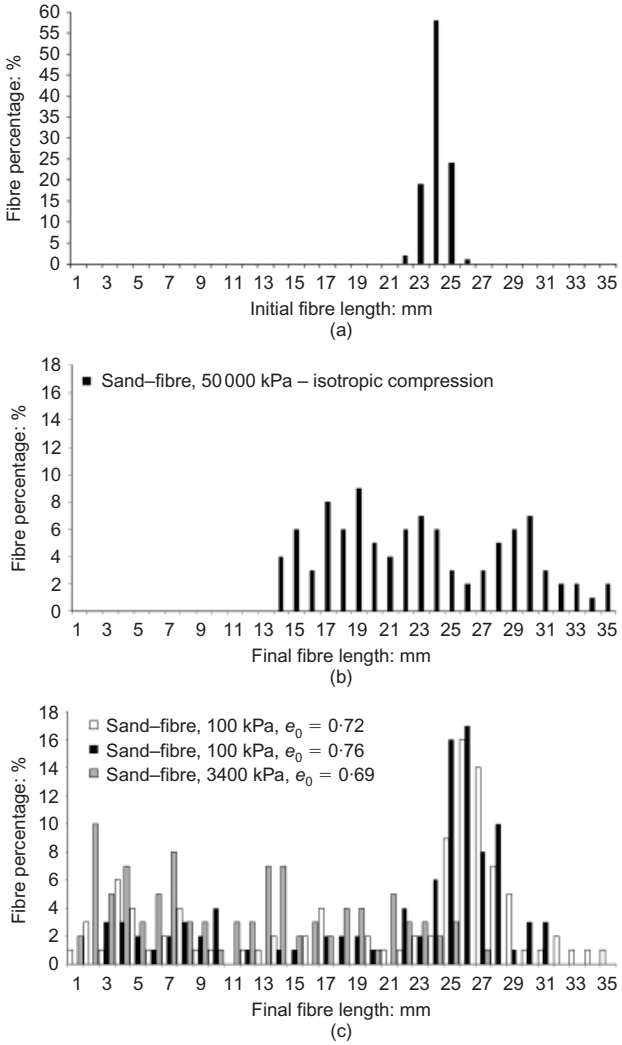

Fig. 5. Evolution of fibre length: (a) initial fibre length; (b) after isotropic compression to 50 MPa; (c) shearing low- and high-pressure tests

to undertake unconfined, presumably because of the added effect of the granular confinement and because of localisation of the tensile strains in the fibres.

Figure 5(c) shows the distribution of fibre lengths after shearing at different confining stresses and initial void ratios. At low stresses (100 kPa), in the denser specimen the fibres suffer more elongation and more breakage than in the looser specimen, which has the higher percentage of fibres that kept intact or almost intact length. The difference is, however, not too significant. Fig. 5(c) also shows a comparison of specimens sheared at 100 kPa and 3400 kPa. There is a clear demarcation between the fibres' behaviour in the two cases: the fibres in the specimen tested at 100 kPa confining stress elongated during shearing, while the fibres in the specimen tested at 3400 kPa seem to have broken into shorter fibres. Some of this breakage might have occurred during the isotropic compression, but since it was not monitored then it is difficult to make a definite conclusion as to the effect of confinement on the fibres' behaviour. If an attempt is made to link this to the stress–strain behaviour and stress–dilatancy observed in Figs 2 and 3, at low confining pressures the elongation shows that the fibres are still working in tension up to the end of shearing, so that their strength is still being mobilised at large strains. This seems to concur with the stress–dilatancy for these tests (Fig. 3(b)), which shows that at low stresses the specimens exhibit

a similar trend to the other tests up to zero compression, after which the sand–fibre composite climbs to a high peak stress ratio with very little dilation. In contrast, the tests carried out at high confining pressure only compress to a critical state ratio almost equal to that for the pure sand. This suggests that either most fibres were broken during compression and did not have much effect on the shearing, or that they were in majority mobilised in tension during shearing, in a similar way to what was observed in the low-stress tests, but that a large proportion were broken by the time the composite reached large strains, and stopped acting effectively as reinforcement.

CRITICAL STATE SOIL MECHANICS APPLIED TO FIBRE-REINFORCED SAND

Critical states in fibre-reinforced sand

Critical state in sands is typically defined by the state reached when stress and density remain constant despite continuing shearing, see, for example, data from Coop & Lee (1993). In addition, crushable sands tend to reach a stable grading at the 'true' critical state, but this is achieved at strains much larger than those typically reached in triaxial tests, for example in ring shear tests (Coop *et al.*, 2004; Muir Wood, 2006). Therefore, the concept of critical state as derived from triaxial test data may be considered as being approximate, even though stress and volume are usually found to stabilise at about 30% strain. In fibre-reinforced sand, there is the additional difficulty that the fibres can deform and break. A 'true' critical state will be reached when sand particles and fibres cease to deform and break. Consoli *et al.* (2007b) carried out ring shear tests on fibre–sand mixtures similar to those tested here, and found that the strength does not deteriorate even at very large strains. Therefore, the critical state determined in terms of stress in the triaxial apparatus should not be too far from the true critical state stress. The difference may arise in the volumetric plane, where additional particle breakage during shearing to true critical state might lead to a reduction in void ratio. Strains that are relevant to geotechnical design rarely reach this magnitude, therefore for the purpose of developing a useful framework, in the analyses presented here it has been necessary to identify representative lines at large strains, where reasonably constant stress and volume were found with continuous shearing. For convenience, in the following they are referred to as $CSL_{sand–fibre}$, and the gradient in $q–p'$ plane to M.

Large strain behaviour: stress plane

The end points for the tests shown in Fig. 2 have been plotted in a $q–p'$ graph in Fig. 6. From Fig. 2, it is clear that the volumetric strain had not stabilised at the end of all tests, but that the tests carried out at low stresses were still dilating at 60% shear strain. The deviatoric stress was, however, found to be constant at the end of nearly all tests, and the end points for these tests provided reliable points to derive a critical state line in the stress plane. Other results from Consoli *et al.* (2007a), on the same composite but for different confining pressures and different stress paths, were used to complement the framework, even though they were systematically stopped at 20% shear strain and did not necessarily reach critical states.

The critical state points for Osorio sand define a straight line, the critical state line (CSL_{sand}), which passes through the origin. Its equation is of the form

$$q = 1{\cdot}22\,p' \tag{5}$$

This is consistent with the critical state ratio $M = 1{\cdot}22$ found from the stress–dilatancy graph (Fig. 3(a)). The large strain points for the sand reinforced with fibres are in agreement with the failure line proposed by Consoli *et al.* (2007a), who reported a bilinear curve up to confining pressures of 680 kPa. Gray & Ohashi (1983), Gray & Al-Refeai (1986) and Maher & Gray (1990) also reported the bilinear failure envelope for other sand–fibre combinations, although steady states were less identifiable from their data. With the addition of the data points obtained from the fibre-reinforced sand tests carried out at up to 3400 kPa confining pressure, it seems that there is convergence of the failure line ($CSL_{sand–fibre}$ in the figure) towards the CSL_{sand}. A simple exponential equation is proposed for the variation of the gradient M of the $CSL_{sand–fibre}$ with stress level. The same equation will be used later in the normalisation of stress paths. In kPa units, the expression for M is

$$M = 1{\cdot}22\left(1 + 0{\cdot}97e^{-(p'/2600)}\right) \tag{6}$$

According to equation (6), $M = 2{\cdot}4$ at $p' = 0$ kPa, $M = 1{\cdot}33$ at $p' = 6000$ kPa, and converges to the value of M for the pure sand ($M = 1{\cdot}22$) at larger stresses.

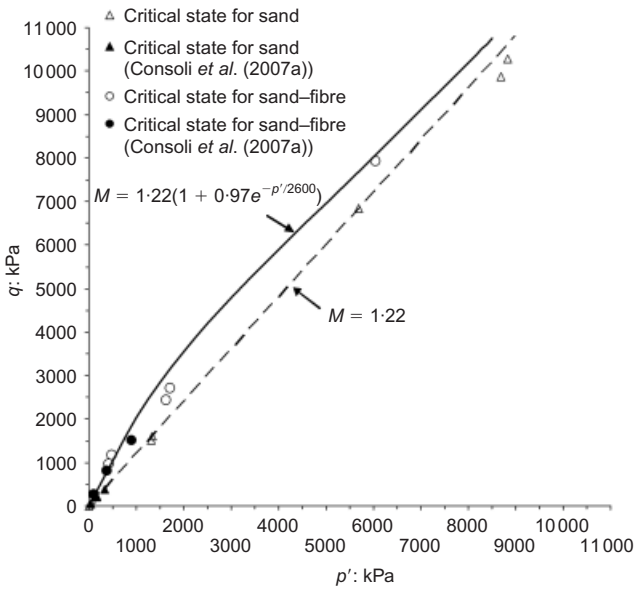

Fig. 6. Critical state envelopes for sand and fibre-reinforced sand in $q–p'$ plane

Large strain behaviour: volumetric plane

The critical state points for the triaxial shearing tests for the unreinforced and large strain points for the fibre-reinforced sand presented in Fig. 2, as well as the points taken from Consoli *et al.* (2007a), have been plotted in a $v–\ln p'$ graph (Fig. 7). The specific volume of each sample was measured using up to three different methods, based on the initial dry unit weight, the final water content and the final unit weight. It was found that the differences in values of void ratio calculated following these three methods were less than 0·04, more often less than 0·02. In each case an average value was taken, having discarded any anomalous values. The specimens that were still showing signs of volumetric variations at the end of the tests are marked with an arrow in the direction of compression/dilation. At pressures up to 1000 kPa, the critical state points for the Osorio sand lie on a curve tending to the maximum void ratio of the material as the pressures reduces ($e_{max} = 0{\cdot}90$). Similar curves have been determined for many other sands, for example Erksak sand (Been *et al.*, 1991), Leighton Buzzard sand (Klotz &

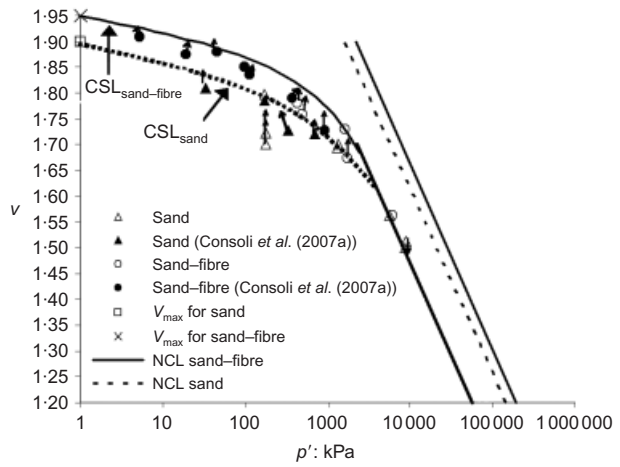

Fig. 7. Critical state line for sand and fibre-reinforced sand

Coop, 2002) and Toyoura sand (Verdugo & Ishihara, 1996). It is hypothesised that at lower stresses the CSL_{sand} and $CSL_{sand–fibre}$ would curve to reach a maximum void ratio determined by the maximum void ratio of the sand and reinforced sand respectively. At higher stresses, the three tests carried out on sand at 3400 kPa (one test) and 5400 kPa (two tests) confining pressure reached stable stress and volumetric conditions, and were considered to have reached critical state. These data points for the higher stresses define a straight line parallel to the NCL_{sand} found by Consoli *et al.* (2005), with an equation

$$v = 2{\cdot}90 - 0{\cdot}156\ln\ p' \tag{7}$$

The specimen of fibre-reinforced sand tested at the high confining pressure of 3400 kPa, which reached stable stress and volume at the end of the test (see Fig. 2(c)), could be assumed to have reached a critical state. The data point for that sample plots very closely to the data points of the pure sand. With the assumption that the CSL will be parallel to the $NCL_{sand–fibre}$, this suggests that the CSL for the reinforced sand at large strains ($CSL_{sand–fibre}$) is coincident with the CSL_{sand}. At lower stresses, however, the data points lie on a curve that seems to tend to the maximum void ratio of the sand–fibre material as pressure reduces, similarly to what was observed in the host sand, but this curved part of the $CSL_{sand–fibre}$, unlike the higher stress straight part, does not seem to coincide with that of the host sand. Instead, it lies above the CSL_{sand} for the Osorio sand. There is no simple explanation as to why this difference exists. A first hypothesis could be drawn for the fact, observed in earlier sections, that the effect of fibre inclusion is more important at lower stress levels and becomes much less significant in terms of volumetric response as the confining stress level gets higher. Second, the value of maximum void ratio for the sand–fibre material appears to be higher than that of the pure sand, but because of the low stresses reached at large strains in those tests, it is not at all certain that the specimens would have reached a critical state anyway. In addition, the apparent convergence of the two CSLs at high stresses in the v–$\ln p'$ plane is not as clear in the q–p' plane, perhaps because fibres are still deforming and breaking at the end of the tests. Thus the identification of a 'true' CSL for the reinforced soil cannot yet be ratified, and the $CSL_{sand–fibre}$ should only be regarded as representative of large strain behaviour.

State boundary surface

The state boundary surface for the non-reinforced and reinforced sand can be determined by normalising the stress path data with respect to an equivalent pressure on a reference line; here the NCL was chosen as reference line. In sands, a state parameter measuring the vertical distance to the NCL is often used (Been & Jefferies, 1985), but a stress state parameter that measures the horizontal distance to the normal compression or CSL has also been successfully used in the past, for example by Klotz & Coop (2001). The latter way of normalising has been traditionally applied by researchers aiming to develop frameworks for the behaviour of soils, for example Cotecchia & Chandler (2000) for structured clays. This is particularly useful for constitutive modelling, when the size of the state boundary surface of the structured soil can be easily related to that of the reconstituted soil (e.g. Baudet & Stallebrass, 2004). The same approach has been adopted here to characterise the effects of fibre reinforcement on the size of the state boundary surface.

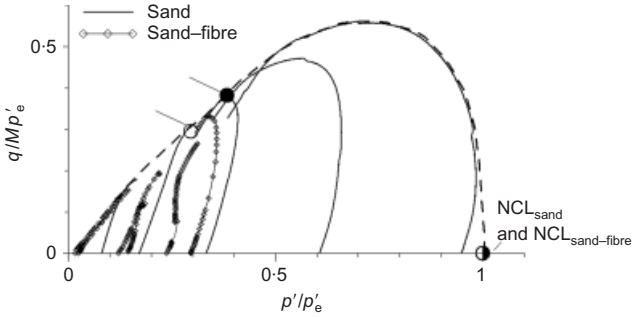

Fig. 8. Normalised stress paths for tests on sand and fibre-reinforced sand

The calculated curves NCL_{sand} and $NCL_{sand–fibre}$, shown in Fig. 1, were used at all levels of pressure to normalise the shearing data. Because of the dependence of the gradient of the $CSL_{sand–fibre}$ with stress level in the q–p' plane, the data have been further normalised by the gradient of the critical state line M, both for the pure sand and the sand–fibre mixture data. The value of M was taken to be constant, equal to 1·22, for the sand. For the reinforced sand, the problem of varying M was solved by adopting the expression proposed in equation (6). The stress paths for the sand and sand–fibre composite, normalised in a q/Mp'_e–p'/p'_e plot, are shown in Fig. 8. Only one pure sand specimen was sheared from a near normally consolidated state, and its stress path starts close to the NCL. All other specimens were sheared from denser states. The points representing the normalised NCLs are shown on the graph. The points representing what should be the normalised CSLs have also been calculated and are plotted. They are in slightly different locations along the $q/Mp'_e = p'/p'_e$ line; the different locations reflect the larger distance between the NCL and CSL of the sand–fibre composite than of the pure sand, which was found from Fig. 7. It is uncertain whether they would coincide had 'true' critical state been determined for the reinforced sand. The state boundary surface appears nevertheless to be unique for the pure sand and sand–fibre material. This suggests that as first approximation, fibre-reinforced sand could be modelled along the same framework as that used for the host sand.

SUMMARY

From the results presented above a clearer picture of the behaviour of the sand–fibre composite can be drawn in relation to that of the host sand. The main points are summarised below.

(*a*) In volumetric space, the NCL of the sand–fibre material lies above that of the host sand, and parallel to it.

(*b*) In volumetric space, there seems to be a CSL for the sand–fibre material which is coincident with that of the host sand at high stresses. At lower stresses, the large strains data seem to curve towards a maximum void ratio, as is observed for the host sand, but it is not clear whether they are also on the CSL. The maximum void ratio for the sand–fibre composite appears to be higher than that for the host sand.

(*c*) In stress space, the gradient of the failure line of the sand–fibre material seems to vary with stress level, possibly due to a change from a slip–yield mechanism to stretching of the fibres. It is initially about twice that of the host sand, tending to the value of the gradient of the CSL of the pure sand at large stresses.

(*d*) The peak strength of the sand–fibre composite does not seem to be linked to volume change, and is reached at low confining pressure with very little dilation.

(*e*) When normalising stress path data for volume and composition, the stress paths for the sand and the sand–fibre composite define a unique state boundary surface, with coinciding NCL. It is not sure whether the normalised CSLs coincide, but this suggests that all differences between the pure and reinforced material could be included in the locations of the NCL and CSL.

ACKNOWLEDGEMENTS

The authors wish to express their gratitude to MCT-CNPq-Brazilian Council of Scientific and Technological Research (projects PNPD #558474/2008-0, Produtividade em Pesquisa #301869/2007-3 and Edital Universal #472851/2008-0) for the financial support to the research group.

REFERENCES

ABNT (Associação Brasileira de Normas Técnicas) (1990). *Soils – maximum void ratio determination for non-cohesive soils*. NBR 12004, Rio de Janeiro, Brazil: ABNT (in Portuguese).

Baudet, B. & Stallebrass, S. E. (2004). A constitutive model for structured clays. *Géotechnique* **54**, No. 4, 269–278, **doi**: 10.1680/geot.2004.54.4.269.

Been, K. & Jefferies, M. G. (1985). A state parameter for sands. *Géotechnique* **35**, No. 2, 99–112, **doi**: 10.1680/geot.1985.35.2.99.

Been, K., Jefferies, M. G. & Hachey, J. (1991). The critical state of sands. *Géotechnique* **41**, No. 3, 365–381, **doi**: 10.1680/geot.1991.41.3.365.

Bishop, A. W. & Wesley, L. D. (1975). A hydraulic triaxial apparatus for controlled stress path testing. *Géotechnique* **25**, No. 4, 657–660, **doi**: 10.1680/geot.1975.25.4.657.

Bueno, B. S., Lima, D. C., Teixeira, S. H. C. & Ribeiro, N. J. (1996). Soil fibre reinforcement: basic understanding. *Proc. Int. Symp. Environ. Geotechnol*., *San Diego* **1**, 878–884.

Burland, J. B. & Symes, M. (1982). A simple axial displacement gauge for use in triaxial apparatus. *Géotechnique* **32**, No. 1, 62–65, **doi**: 10.1680/geot.1982.32.1.62.

Casagrande, M. D. T. (2005). *Behavior of fiber-reinforced soils under large shear strains*. PhD thesis, Federal University of Rio Grande do Sul, Porto Alegre, Brazil (in Portuguese).

Casagrande, M. D. T., Coop, M. R. & Consoli, N. C. (2006). The behavior of a fiber-reinforced bentonite at large shear displacements. *J. Geotech. Geoenviron. Engng, ASCE* **132**, No. 11, 1505–1508.

Consoli, N. C., Ulbrich, L. A. & Prietto, P. D. M. (1997). Engineering behavior of random distributed fiber-reinforced cement soil. *Proceedings of international symposium on developments in soil and pavement mechanics*, pp. 481–486. Rotterdam: A. A. Balkema.

Consoli, N. C., Prietto, P. D. M. & Ulbrich, L. A. (1998). Influence of fiber and cement addition on behavior of sandy soil. *J. Geotech. Geoenviron. Engng, ASCE* **124**, No. 12, 1211–1214.

Consoli, N. C., Prietto, P. D. M. & Ulbrich, L. A. (1999). The behavior of a fiber-reinforced cemented soil. *Ground Improvement, ISSMGE* **3**, No. 3, 21–30.

Consoli, N. C., Montardo, J., Prietto, P. D. M. & Pasa, G. (2002). Engineering behavior of a sand reinforced with plastic waste. *J. Geotech. Geoenviron. Engng, ASCE* **128**, No. 6, 462–472.

Consoli, N. C., Casagrande, M. D. T., Thomé, A. & Prietto, P. D. M. (2003a). Plate load test on fiber-reinforced soil. *J. Geotech. Geoenviron. Engng, ASCE* **129** , No. 10, 951–955.

Consoli, N. C., Vendruscolo, M. A. & Prietto, P. D. M. (2003b). Behavior of plate load tests on soil layers improved with cement and fiber. *J. Geotech. Geoenviron. Engng, ASCE*, **129**, No. 1, 96–101.

Consoli, N. C., Heineck, K. S. & Casagrande, M. D. T. (2003c). Large strain behaviour of polypropylene fiber-reinforced sandy soil. *Proc. 12th Pan-Am. Conf. Soil Mech. Geotech. Engng, Boston, USA* **2**, 2201–2206.

Consoli, N. C., Montardo, J., Donato, M. & Prietto, P. D. M. (2004). Effect of material properties on the behavior of sand–cement–fibre composites. *Ground Improvement, ISSMGE* **8**, No. 2, 77–90.

Consoli, N. C., Casagrande, M. D. T. & Coop, M. R. (2005). Effect of fiber reinforcement on the isotropic compression behavior of a sand. *J. Geotech. Geoenviron. Engng, ASCE* **131**, No. 11, 1434–1436.

Consoli, N. C., Heineck, K. S., Casagrande, M. D. T. & Coop, M. R. (2007a). Shear strength behavior of fiber-reinforced sand considering triaxial tests under distinct stress paths. *J. Geotech. Geoenviron. Engng , ASCE* **133**, No. 11, 1466–1469.

Consoli, N. C., Casagrande, M. D. T. & Coop, M. R. (2007b). Performance of a fibre-reinforced sand at large shear strains. *Géotechnique* **57**, No. 9, 751–756, **doi**: 10.1680/geot.2007.57.9.751.

Consoli, N. C., Casagrande, M. D. T., Thomé, A., Dalla Rosa, F. & Fahey, M. (2009a). Effect of relative density on plate tests on fibre-reinforced sand. *Géotechnique*, **59**, No. 5, 471–476, **doi**: 10.1680/geot.2007.00063.

Consoli, N. C., Festugato, L. & Heineck, K. S. (2009b). Strain-hardening behaviour of fibre-reinforced sand in view of filament geometry. *Geosynthetics Int*. **16**, No. 2, 109–115.

Coop, M. R. & Lee, I. K. (1993). The behaviour of granular soils at elevated pressures. *Proceedings of the Wroth memorial symposium: predictive soil mechanics*, pp. 186–198. London: Thomas Telford.

Coop, M. R., Sorensen, K. K., Bodas Freitas, T. & Georgoutsos, G. (2004). Particle breakage during shearing of a carbonate sand. *Géotechnique* **54**, No. 3, 157–163, **doi**: 10.1680/geot.2004.54.3.157.

Cotecchia, F. & Chandler, R. J. (2000). A general framework for the mechanical behaviour of clays. *Géotechnique* **50**, No. 4, 431–447, **doi**: 10.1680/geot.2000.50.4.431.

Crockford, W. W., Grogan, W. P. & Chill, D. S. (1993). Strength and life of stabilized pavement layers containing fibrillated polypropylene. *Transpn Res. Rec*. **1418**, 60–66.

Cuccovillo, T. & Coop, M. R. (1999). On the mechanics of structured sands. *Géotechnique* **49**, No. 6, 741–760, **doi**: 10.1680/geot.1999.49.6.741.

Diambra, A., Ibraim, E., Muir Wood, D., Bennanni, Y. & Russell, A. (2008). Effect of sample preparation on the behaviour of fibre reinforced sands. *Proc. IS Atlanta 08: Deformation Characteristics Geomater*. **2**, 629–636.

Gray, D. H. & Al-Refeai, T. (1986). Behavior of fabric versus fiber-reinforced sand. *J. Geotech. Engng, ASCE* **112**, No. 8, 804–826.

Gray, D. H. & Maher, M. H. (1989). Admixture stabilization of sands with random fibers. *Proc. 12th Int. Conf. Soil Mech. Found. Engng, Rio de Janeiro* **2**, 1363–1366. Rotterdam: A. A. Balkema.

Gray, D. H. & Ohashi, H. (1983). Mechanics of fiber-reinforcement in sand. *J. Geotech. Engng, ASCE* **109**, No. 3, 335–353.

Gudehus, G. (1996). A comprehensive constitutive equation for granular materials. *Soils Found*. **36**, No. 1, 1–12.

Heineck, K. S., Coop, M. R. & Consoli, N. C. (2005). Effect of microreinforcement of soils from very small to large shear strains. *J. Geotech. Geoenviron. Engng, ASCE* **131**, No. 8, 1024–1033.

Jefferies, M. & Been, K. (2000). Implications for critical state theory from isotropic compression of sand. *Géotechnique* **50**, No. 4, 419–429, **doi**: 10.1680/geot.2000.50.4.419.

Klotz, E. U. & Coop, M. R. (2001). An investigation of the effect

of soil state of the capacity of driven piles in sands. *Géotechnique* **51**, No. 9, 733–751, **doi**: 10.1680/geot.2001.51.9.733.

Klotz, E. U. & Coop, M. R. (2002). On the identification of critical state lines for sands. *Geotech. Testing J.*, *ASTM* **25**, No. 3, 289–302.

Maeda, K. & Ibraim, E. (2008). DEM analysis of 2D fiber-reinforced granular soils. *Proc. 4th Int. Symp. Deformation Characteristics Geomater.*, *Atlanta, Georgia* **2**, 623–628.

Maher, M. H. & Gray, D. H. (1990). Static response of sands reinforced with randomly distributed fibers. *J. Geotech. Engng, ASCE* **116**, No. 11, 1661–1677.

Maher, M. H. & Ho, Y. C. (1993). Behavior of fibre-reinforced cemented sand under static and cyclic loads. *Geotech. Testing J.*, *ASTM* **16**, No. 3, 330–338.

Maher, M. H. & Ho, Y. C. (1994). Mechanical properties of kaolinite/fiber soil composite. *J. Geotech. Engng, ASCE* **120**, No. 8, 1381–1393.

Muir Wood, D. (2006). Geomaterials with changing grading: a route towards modelling. *Proceedings of the international symposium on geomechanics and geotechnics of particulate media, Ube, Yamaguchi, Japan*: *Geomechanics and geotechnics of particulate media* (eds M. Hyodo, H. Murata, and Y. Nakata), pp. 313–325. London: Taylor & Francis Group.

Nataraj, M. S., Addula, H. R. & McManis, K. L. (1996). Strength and deformation characteristics of fiber reinforced soils. *Proc. 3rd Int. Symp. Environ. Geotechnol.*, *San Diego, Pennsylvania* **1**, 826–835. Technomic Publishing Co.

Pestana, J. M. & Whittle, A. J. (1999). Formulation of a unified constitutive model for clays and sands. *Int. J. Numer. Analyt. Meth. Geomech*. **23**, No. 12, 1215–1243.

Ranjan, G. R. & Charan, H. D. (1996). Probabilistic analysis of randomly distributed fiber- reinforced soil. *J. Geotech. Engng, ASCE*, **122**, No. 6, 419–426.

Santoni, R. L., Tingle, J. S. & Webster, S. L. (2001). Engineering properties of sand–fiber mixtures for road construction. *J. Geotech. Geoenviron. Engng, ASCE* **127**, No. 3, 258–268.

Santos, A. P. S. (2008). *Study of the behaviour of fibre-reinforced cemented sand under high pressures*. PhD thesis, Federal University of Rio Grande do Sul, Porto Alegre, Brazil (in Portuguese).

Schofield, A. W. & Wroth, C. P. (1968). *Critical state soil mechanics*. London: McGraw-Hill.

Shewbridge, E. & Sitar, N. (1989). Deformation characteristics of reinforced sand in direct shear. *J. Geotech. Engng, ASCE* **115**, No. 8, 1134–1147.

Specht, L. P., Ceratti, J. A. P. & Consoli, N. C. (2006). A laboratory study of soil–cement–fiber mixtures under static and repeated loadings for pavements. *Int. J. Pavements* **5**, No. 1, 99–108.

Stauffer, S. D. & Holtz, R. D. (1996). Stress–strain and strength behavior of staple fiber and continuous filament-reinforced sand. *Transpn Res. Rec*. **1474**, 82–95.

Verdugo, R. & Ishihara, K. (1996). The steady state of sandy soils. *Soils Found*. **36**, No. 2, 81–89.